Applied Problems of Nonlinear Oscillation and Wave Theory

Izvestiya Vysshikh Uchebnykh Zavedeniy. Applied Nonlinear Dynamics. 2022;30(4)

Article DOI: 10.18500/0869-6632-2022-30-4-391-410

Reconstruction of integrated equations of periodically driven phase-locked loop system from scalar time series

M. V. Sysoeva[1,2]✉, *M. V. Kornilov*[1,3,4], *L. V. Takaishvili*[3], *V. V. Matrosov*[4], *I. V. Sysoev*[1,3,4]

[1]Saratov Brunch of Kotelnikov Institute of Radioengineering and Electronics of RAS, Russia
[2]Yuri Gagarin State Technical University of Saratov, Russia
[3]Saratov State University, Russia
[4]Lobachevsky State University of Nizhny Novgorod, Russia
E-mail: ✉bobrichek@mail.ru, kornilovmv@gmail.com, nar7187@yandex.ru, matrosov@rf.unn.ru, ivssci@gmail.com
Received 22.10.2021, accepted 14.12.2021, published 1.08.2022

Abstract. *Purpose* of this work is to develop a reconstruction technique for the equations of a phase-locked loop system under periodic external driving from a scalar time series of one variable. *Methods.* Instead of the original model, we reconstructed a time-integrated model. So, since it is not necessary to evaluate the second derivative of the observable numerically, the method sensitivity to observation noise has significantly decreased. The external periodic driving is approximated with a trigonometric polynomial of time, the antiderivative of which is also a trigonometric polynomial. The assumption about continuity of an unknown nonlinear function is used to construct the target function for optimization. *Results.* It is shown that the proposed approach gives a significant advantage over the previously developed approach to the reconstruction of non-integrated equations, allowing to achieve acceptable parameter estimates with measurement noise being about 10% of the RMS deviation of the signal even in the presence of external driving. *Conclusion.* The described approach significantly extends the possibilities of reconstruction of phase-locked loop systems, allowing systems to be reconstructed under arbitrary periodic driving and at the same time significantly increasing noise resistance.

Keywords: reconstruction, phase-locked loop system, periodic driving.

Acknowledgements. This study was supported in part by the President of the Russian Federation under Grant MD-3006.2021.1.2, and in part by the Russian Foundation for Basic Research, grant No. 19-02-00071.

For citation: Sysoeva MV, Kornilov MV, Takaishvili LV, Matrosov VV, Sysoev IV. Reconstruction of integrated equations of periodically driven phase-locked loop system from scalar time series. Izvestiya VUZ. Applied Nonlinear Dynamics. 2022;30(4):391–410. DOI: 10.18500/0869-6632-2022-30-4-391-410

Introduction

The theoretical possibilities of methods based on the reconstruction of equations over time series are very large [1]: indirect measurement of quantities and even whole functions that cannot be measured directly; clustering of objects according to model parameters; verification

of different models of the same object or phenomenon; prediction of future behavior in time or prediction of behavior with a small changing parameters (bifurcation forecast). In the application to biological neurons, all these possibilities are in demand. Since direct measurements of most model parameters are impossible, the experiments themselves are traumatic for the cell. It is very important to be able to identify cells and use their signals to determine which type a particular cell belongs to. However, progress in this area in recent years has not been very great. This is due to a number of factors: imperfection of models, noise and interference during measurement. To date, none of the known mathematical models of neurons (Hodgkin–Huxley [2], Fitzhugh–Nagumo [3, 4], Hindmarsh–Rose [5], Morris–Lekar [6]) failed to reconstruct the equations from experimental time series of cellular activity of real neurons. One of the main reasons for this is the need to measure all model variables in an experiment. However, this is not possible, since some of the models are conditional. In fact, the only measurable variable is the transmembrane potential. There are several approaches to get the remaining variables (hidden). Either they are obtained by numerical differentiation or integration, as proposed in [7], or by the method of time delays, as in [8], or it is necessary to set initial guesses for them and then adjust the series themselves together with unknown parameters and nonlinear functions to the observed ones (this approach is called methods of working with hidden variables [9]).

The time delay method is suitable in two cases: if the equations for the object are completely unknown and any approach to the reconstruction of the state vector is suitable, or when reconstructing systems with a delay, if the lagging variable is the only one (if the equation is of the second order, you have to resort to a combination of delays and numerical differentiation [10]). To reconstruct the equations of neurons written for biophysical reasons, this method is not suitable, since it is impossible to get the missing variables by shifting — they have a different meaning and a different dimension. Numerical differentiation and integration are used either when nothing is known about the equations for the object [7], or when the equations are composed in such a way that one of the variables has, for example, the physical meaning of the coordinates, and the other — velocity (charge — current, etc., etc.). For neuron models [2, 3, 5, 6] this is not applicable due to their device. But some other models of biological systems allow us to reconstruct some of the variables from the model of the vocal cords observed in this way [11] or the nephron [12]. The most significant successes in this area are associated with the use of statistical estimates [13].

In addition to models of neurons built for biophysical reasons, there are also models of generators capable of demonstrating a wide variety of behavioral modes characteristic of the activity of neurons. One of these generators was originally proposed for communication purposes. It is a phase-locked loop (PLL) system with a bandpass filter [14]. Modes of neuropodic generation, including periodic and chaotic bursts of pulses, were found in the model in the works [15, 16]. Then they were demonstrated experimentally [17]. The PLL system is not a neuron model. Therefore, it will not be possible to verify it according to the activity of a biological neuron or evaluate physiologically significant parameters of a neuron with its help. But it can be useful for clustering neurons and for detecting connections between them. This is already enough for the solution of the problem of reconstructing this system according to experimental data to be justified. Its advantage is that for this system, one of the two missing variables can be obtained by numerical differentiation, and the second by numerical integration of the observable.

Earlier, based on the approach proposed in [18] for first-order oscillators with a delay in their own dynamics, in [19], a method was constructed for reconstructing one autonomous PLL system with a bandpass filter, which also has a delay in the variable y. Further, a similar approach was extended to the ensemble of linked PLL [20] without delay. However, for the practical application of the approach, the developments presented in [19, 20] are not enough, since they have a number of significant drawbacks. Firstly, the proposed technique is quite sensitive to noise:

in a numerical experiment, it was possible to reconstruct the dynamics in the ensemble only in the presence of additive noise of the order of 1%. In a real experiment with extracellular recordings of neurons, the noise level is much higher [21]. Despite the use of smoothing polynomials for numerical differentiation, the need to obtain the second derivative of the observed does not make it possible to achieve the operability of the method with noticeably large noises. Secondly, the methodology proposed in [19, 20] operates when evaluating a nonlinear function with terms of the type v/y or $v/y(t - \mathsf{t})$, where v is some well—known expression depending on the observed y and its first and second the derivative, and the argument $t - \mathsf{t}$ means that in this case the time-delayed value of the observable is used. Such terms give a singularity at $y \; ! \; 0$. Since in the experiment y is measured with errors caused by noise, all the results for $jyj < \mathsf{m}$, where the value of m has to be selected empirically, turn out to be unreliable. Small values of y are typical for quite long periods of time, especially in excitable mode. because of this, most of the time series is excluded from consideration, and for some modes, the nonlinear function can only be partially reconstructed at all. Thirdly, the methodology proposed in [19] works only for a solitary system, which is almost meaningless when reconstructing from biological data: individual cells are silent and generate nothing, and when reconstructing related cells using the methodology from [20], it is necessary to have rows of all.

The purpose of this work is to expand the scope of the PLL reconstruction technique with a bandpass filter for its further application to experimental time series of real neurons. In order to eliminate the above disadvantages, a transition has been made from the initial equations described in [15, 16] to time-integrated equations. The external impact will be approximated by a trigonometric polynomial of degree P, as it was proposed for systems of another type in [22].

1. Mathematical model of the PLL system

The dynamics of the phase-controlled generator considered here in the presence of external influence $I_{\text{ext}}(t)$ is described by a non-autonomous system of third-order ordinary differential equations defined in a cylindrical phase space $(\mathsf{3} \bmod 2\mathsf{p}, y, z)$:

$$\begin{aligned} \frac{d\mathsf{3}}{dt} &= y, \\ \frac{dy}{dt} &= z, \\ \varepsilon_1\varepsilon_2\frac{dz}{dt} &= \mathsf{g} + I_{\text{ext}}(t) - (\varepsilon_1 + \varepsilon_2)z - (1 + \varepsilon_1\cos\mathsf{3})y. \end{aligned} \tag{1}$$

In terms of the phase-locked frequency system $\mathsf{3}$ — the current phase difference of the tuned and reference oscillator, g — initial frequency detuning, $\varepsilon_1, \varepsilon_2$ — the inertia parameters of the filters. Applied to the dynamics of a neuron, the variable y can be interpreted as describing a change in the membrane potential. The parameters ε_1 and ε_2 allow you to set the necessary dynamic mode, g — the external ion current in the intercellular substance is constant at the measurement time (slowly changing component [2]), I_{ext} — periodic exposure to another neuron or external electrical stimulation. If I_{ext} has a nonzero constant component (shift), it is actually taken into account as part of the parameter g.

In [23] it was shown that this generator is able to demonstrate various dynamic modes that are characteristic of neurons: regular pulse dynamics (spikes), burst oscillations (bursts) with a different number of pulses in a bundle. In the work [15], the plane of the model parameters was divided into the regions of existence of the corresponding dynamic modes: quasi-regular oscillations, oscillations with a different number of pulses in a bundle, chaotic oscillations. In the

work [24], the model of the generator under consideration, which is in an excitable state, is studied in detail. In this model, responses appear only when an external influence is applied. The presence of an excitable mode is very important, since the neurons of the brain are in an excitable state most of the time. It is shown that for $\mathsf{g} = 0$ and $I_{\text{ext}}(t) = 0$ in the system (1) there is a continuum of equilibrium states $(\mathsf{3}^*, 0, 0)$ located on the segment $\mathsf{3}^*\ \mathit{2}\ [-\arccos(1/\varepsilon_1); \arccos(1/\varepsilon_1)]$, one of which eventually turns out to be a system (1) with non-zero initial values of y and z. It is possible to force the system to generate pulses at $\mathsf{g} = 0$ by applying an external pulse action $I_{\text{ext}}(t)$ — harmonic action in such a system with such parameters leads to forced harmonic oscillations. In [25], the influence of periodic stimulation parameters on the response of the studied generator is considered. Various methods of evaluating the generator responses to external excitation showed that the response significantly depends on the amplitude of the stimulating pulses and depends less on the period of their repetition; this is confirmed by the results of the Poisson random sequence.

2. The method of reconstruction of the integrated equations of the PLL system

In the hardware implementation of the PLL system [17], it is possible to measure a single variable y. It also corresponds to the transmembrane potential recorded in a biological experiment from individual neurons [26, 27]. Therefore, the problem of reconstructing the equations (1) was immediately formulated in such a way that only the variable y is measured. Following the work of [19], the variable $\mathsf{3}$ was restored by numerical integration by the Simpson method, the variable z — by numerical differentiation using a polynomial approximating by m points (Savitsky filter–Golay [28]). For reconstruction using noiseless or low-noise implementations, the smallest $m = 3$ is suitable. In the presence of noise, m can be selected using the quality of reconstruction of a nonlinear function as a criterion, as was done in [19]. The method proposed in [19, 20] also required numerically obtaining the second derivative of the observed — time series of the value dz/dt, which was the main reason for its low noise resistance. The algorithm proposed below does not require numerical calculation of the second derivative. The variable $\mathsf{3}$ can be restored by numerical integration by the Simpson method. Since the method uses the construction of parabolas at intervals equal to two sampling times, then an odd number of points in the measured series (N) will always be considered: if necessary, one value can always be discarded without significant loss of information.

To increase the generality and applicability of the method to experimental data, it is necessary to make the reconstructed model more general. To do this, we will rewrite the last equation of the system (1) in the form (2), where the function f does not have to correspond to the formula (3) (in a real system it almost certainly does not correspond), that is, the reconstruction method we will write immediately for an arbitrary continuous function f.

$$\frac{dz}{dt} = \frac{\mathsf{g}}{\varepsilon_1\varepsilon_2} + \frac{1}{\varepsilon_1\varepsilon_2} I_{\text{ext}}(t) - \frac{\varepsilon_1 + \varepsilon_2}{\varepsilon_1\varepsilon_2} z - f(\mathsf{3})y, \tag{2}$$

$$f(\mathsf{3}) = \frac{1 + \varepsilon_1 \cos \mathsf{3}}{\varepsilon_1\varepsilon_2}. \tag{3}$$

Next, we integrate the last equation of a separate oscillator (2) in time and introduce additional designations a_0 and a_1 similarly to [20]:

$$z = \mathsf{a}_0 t + \mathsf{a}_1 y - \int f(\mathsf{3}) \frac{d\mathsf{3}}{dt} dt + \int I^{\mathsf{0}}_{\text{ext}}(t) dt, \tag{4}$$

$$\mathsf{a}_0 = \frac{\mathsf{g}}{\varepsilon_1 \varepsilon_2}, \quad \mathsf{a}_1 = -\frac{\varepsilon_1 + \varepsilon_2}{\varepsilon_1 \varepsilon_2}, \quad I^{\mathsf{0}}_{\text{ext}} = \frac{I_{\text{ext}}}{\varepsilon_1 \varepsilon_2}, \tag{5}$$

where we used the fact that $\int z dt = y$, $\int (dz/dt) = z$. Next, we will introduce into consideration a new nonlinear function $\mathsf{F}(\mathsf{3})$, which will be smooth, since by definition its first derivative is $f(\mathsf{3})$, for which we have agreed that it is continuous.

$$\int f(\mathsf{3}) \frac{d\mathsf{3}}{dt} dt = \int f(\mathsf{3}) d\mathsf{3} = \mathsf{F}(\mathsf{3}). \tag{6}$$

Also note that the integration constant in the equation (4) can be entered into $\mathsf{F}(\mathsf{3})$ without loss of generality.

Following the ideas of [18], we will build an objective function for calculating the coefficients a_0 and a_1, based on minimizing the length of the description of the nonlinear function F. This will eliminate the explicit decomposition of the function f and its primitive F in a row and at the same time increase the generality of the method (it can be used for arbitrary f) and reduce parameterization (the number of parameters to be evaluated a). This will improve the statistical properties of the estimates of the coefficients remaining in the model: the fewer parameters, the better their estimates. The external effect, following [22], is represented as a trigonometric polynomial, where the frequency $\mathsf{W} = 2\mathsf{p}/T_{\mathbf{ext}}$ is known. The question of how to pick it up, we will analyze further. Thus, the following expression for the nonlinear function F obtained from the equation (4) becomes the basic one for us:

$$\mathsf{F}(\mathsf{3}) = \mathsf{a}_0 t + \mathsf{a}_1 y + \sum_{k=1}^{k=K} \left(\mathsf{a}_{2k} \cos(k\mathsf{W}t) + \mathsf{a}_{2k+1} \sin(k\mathsf{W}t) \right) - z, \tag{7}$$

where K is the degree of the trigonometric polynomial. The constant term in the formula (7) is not necessary: it, like the integration constant, is included in F; that is, in fact, F can be determined up to a constant, but this is natural, since F is a primitive f.

Next, we will conduct all calculations, following the work of [20]. However, we will keep in mind a new expression for a nonlinear function (7). Let's introduce a sorting mapping $Q(n)$, where n is the number of a point in a series, matching the nth point in the original series with its number $Q(n)$ in ascending order $\mathsf{3}$. Let's also consider the inverse mapping Q^{-1}, which calculates by number in the sorted series the number in the original one, so that $Q^{-1}(Q(n)) = n$. Consider the point located in the sorted series immediately before $Q(n)$th. Then in the original series it has the number $Q^{-1}(Q(n) - 1)$, which we denote as p_n for brevity. Increment d_n of the function F on the segment $[\mathsf{3}(p_n); \mathsf{3}(n)]$ will be expressed by the formula (8):

$$
\begin{aligned}
\mathsf{d}_n = \mathsf{F}(\mathsf{3}(n)) - \mathsf{F}(\mathsf{3}(p_n)) &= \mathsf{a}_0 \mathsf{D}t(n) + \mathsf{a}_1 \mathsf{D}y(n) - \mathsf{D}z(n) + \sum_{k=1}^{k=K} \left(\mathsf{a}_{2k} \mathsf{D}\mathsf{J}_k + \mathsf{a}_{2k+1} \mathsf{D}\mathsf{X}_k\right), \\
\mathsf{D}t(n) &= t(n) - t(p_n), \\
\mathsf{D}y(n) &= y(n) - y(p_n), \\
\mathsf{D}z(n) &= z(n) - z(p_n), \\
\mathsf{D}\mathsf{J}_k &= \cos(k\mathsf{W}t(n)) - \cos(k\mathsf{W}t(p_n)), \\
\mathsf{D}\mathsf{X}_k &= \sin(k\mathsf{W}t(n)) - \sin(k\mathsf{W}t(p_n)).
\end{aligned} \tag{8}
$$

At the same time, the value of n, at which $Q(n) = 0$ (we will continue to assume that the numbering starts from zero, that is, $n = 0.1, \ldots, N - 1$), is not acceptable, since there is no corresponding p_n for it (no the previous point in the sorted series is our smallest value). As an objective function, consider the value L:

$$
L(\mathsf{a}_0, \mathsf{a}_1, \ldots, \mathsf{a}_{2K+1}) = \sum_n \mathsf{d}_n^2. \tag{9}
$$

It is obvious from (8) that L will depend on $\mathsf{a}_k j_{k=0,\ldots,2K+1}$ is quadratic. The formula (9) can be considered as a formulation of the least squares problem for approximating the values of $\mathsf{D}z(n)$. Expressions with coefficients a_k are basic functions (more precisely, their values available at the time of measurements), and d_n correspond to residuals. With the correct choice of a_k, the objective function L will be much smaller than with the wrong one, when the coefficients a_k are incorrectly defined and the function f has gaps at almost every point.

Since even with the correct choice of a_k in the general case $L > 0$, then with a finite N the estimates obtained in this way must be biased — their mathematical expectation will not exactly coincide with the true values. Since the function F is not only continuous, but also differentiable (by definition, it is the prototype of the continuous function f) on the half-interval $0 \; 6 \; 3 < 2\mathsf{p}$, then $\mathsf{d}_n \;\; ! \;\; d\mathsf{F}(\mathsf{3}(p_n))$, d_n is an approximation of the differential of the function F at the point $\mathsf{3}(p_n)$ on the right or at the point $\mathsf{3}(n)$ on the left, and for a differentiable function in the limit it is the same. Then the following relation must be fulfilled:

$$
\lim_{N \; ! \; 1} L = \int_0^{2\mathsf{p}} (d\mathsf{F})^2 = \int_0^{2\mathsf{p}} \left(\frac{d\mathsf{F}}{d\mathsf{3}}\right)^2 (d\mathsf{3})^2 = \left(\frac{d\mathsf{F}}{d\mathsf{3}}\right)^2 d\mathsf{3}\Bigg|_0^{2\mathsf{p}} = 0. \tag{10}
$$

Thus, the estimates by the proposed method are asymptotically unbiased.

The proposed approach allows us to estimate the values of a_0 and a_1, which are combinations of the original parameters g, ε_1 and ε_2, but not these parameters themselves. If we consider the third equation of the system (1), we can see that when replacing $1 + \varepsilon_1 \cos \mathsf{3} = f(\mathsf{3})$ it will be impossible to evaluate separately g, ε_1 and ε_2, because all the terms of the equation, including the right part, stand with unknown coefficients (or functions). Thus, the system of equations for determining the coefficients that could be compiled would be degenerate (there is no free term). This means that there is no other way to evaluate g, ε_1 and ε_2 separately according to the data. This limitation is a property of the system, not a disadvantage of the method.

The described algorithm assumes knowledge of the period of external influence. Even a small error in its value will greatly affect the reconstruction results, as it was shown in [29]. The simplest and most effective solution to this problem with modern computing tools is to iterate

over the values of the trial period of the impact of $\tilde{T}$ in a rather large range with a step of h of the order of the sampling step. In this case, the integer ratio between T and h is not necessary. By the minimum of the constructed dependency $L(\tilde{T})$ it is possible to estimate the true period fairly accurately. Relying on the results of [22], we can expect that the high sensitivity of the objective function to the exposure period in a typical case will ensure the correct determination of the period even with low values of the degree of the trigonometric polynomial P and insufficient smoothing of m in the fight against measurement noise.

The proposed approach also makes it possible to reconstruct the external impact based on estimates of the $\mathsf{a}_k\mathsf{j}_{k=2,\ldots,2K+1}$ up to a multiplier of $1/(\varepsilon_1\varepsilon_2)$, which in general cannot be determined. To do this, you need to differentiate the incoming (7) trigonometric polynomial:

$$I^0_{\text{ext}}(t) = \sum_{k=1}^{k=K} \big(- k\mathsf{W}\mathsf{a}_{2k} \sin(k\mathsf{W}t) + k\mathsf{W}\mathsf{a}_{2k+1} \cos(k\mathsf{W}t)\big). \tag{11}$$

Since the values of the coefficients are $\mathsf{a}_k\mathsf{j}_{k=2,\ldots,2K+1}$ and the frequency value of W are known, the external impact by the formula (11) can be calculated for any time t.

After receiving the values of a_k, it can be tabulated using the formula (7) function F. Tabular, because in the formula (7) includes the values of y and z, and these variables are available only at the moments of measurement. But the F function itself is not very interesting. For the reconstruction of the model, its primitive $f(\mathsf{3})isinteresting$. How can one analytically integrate (7) by $\mathsf{3}$ — not clear. Therefore, it is easier to express f from the formula (2) by substituting expressions for a_0 and a_1 from (4) there:

$$f(\mathsf{3}) = \left(\mathsf{a}_0 + \mathsf{a}_1 z + I^0_{\text{ext}}(t) - \frac{dz}{dt}\right) \Big/ y. \tag{12}$$

Calculation by the formula (12) is possible only for $\mathsf{3}$ corresponding to the observed y (otherwise there will be no values of y, z and dz/dt). At the same time, there are two limitations that the rest of the algorithm lacks. These limitations were inherent in the original method proposed in [19]: firstly, it is necessary to numerically calculate the second derivative of the observable, since $dz/dt = d^2y/dt^2$; secondly, at $y \approx 0$ the calculated values will be highly inaccurate, especially in the presence of noise. It should be noted that even despite these limitations, the estimates obtained will be noticeably more accurate than using the original approach from [19], since the coefficients a_k were calculated without relying on the estimate dz/dt and without restrictions for $y \approx 0$.

3. Results

3.1. Generating series and restoring the state vector. The equations (1) were solved by the Euler method. The sampling interval $\mathsf{D}t = 1/32$, equal to the integration step, was selected empirically in such a way as to obtain a stable solution. A detailed study of this issue was conducted at [30].

To test the method, the PLL system was considered in two modes: excitable ($\mathsf{g} = 0, \varepsilon_1 = 4, \varepsilon_2 = 10$) and oscillatory ($\mathsf{g} = 0.075, \varepsilon_1 = 4.5, \varepsilon_2 = 10$ — spike mode according to the classification [20]). Three types of effects were applied: rectangular pulses, Gaussian pulses and harmonic effects. Pulse action of both types in both modes (Fig. 1, *c*, *e*), and harmonic - only for oscillatory mode (Fig. 1, *a*). The choice of impact types is due to the fact that harmonic impact is the easiest to describe and it is the easiest to test the method on it. Gaussian pulses are required to describe trigonometric polynomials of high orders. Being smooth, they can still be described

satisfactorily, and rectangular pulses are typical in radio engineering and were considered for this PLL system in [25]. If the system is in a subthreshold mode, then under harmonic influence it demonstrates forced linear oscillations — the mode is both meaningless from the point of view of neurodynamics and inconvenient for reconstruction, since it contains too little information.

In accordance with the work of [25], we introduce the notation we introduce the notation: A_{sp} — the amplitude of the stimulating pulse, t_{sp} — the duration of the input pulse, T_{sp} — the period of stimulation. In order to maintain the same power of external influence for its different forms, the following parameters were used:

1. for rectangular pulses $A_{\text{sp}} = 0.26$, $T_{\text{sp}} = 100$, $\mathsf{t}_{\text{sp}} = 10$, duty cycle $Q_{\text{sp}} = T_{\text{sp}}/\mathsf{t}_{\text{sp}} = 10$;
2. for Gaussian pulses $A_{\text{gp}} = A_{\text{sp}}\sqrt{2} = 0.26$, $T_{\text{gp}} = T_{\text{sp}} = 100$, $\mathsf{t}_{\text{gp}} = \mathsf{t}_{\text{sp}}/\sqrt{2}$;
3. for harmonic effects $A_{\text{h}} = A_{\text{sp}}\sqrt{2}/Q_{\text{sp}}$, $T_{\text{h}} = T_{\text{sp}} = 100$.

Measuring noise with a standard deviation of 10% from the standard deviation of the

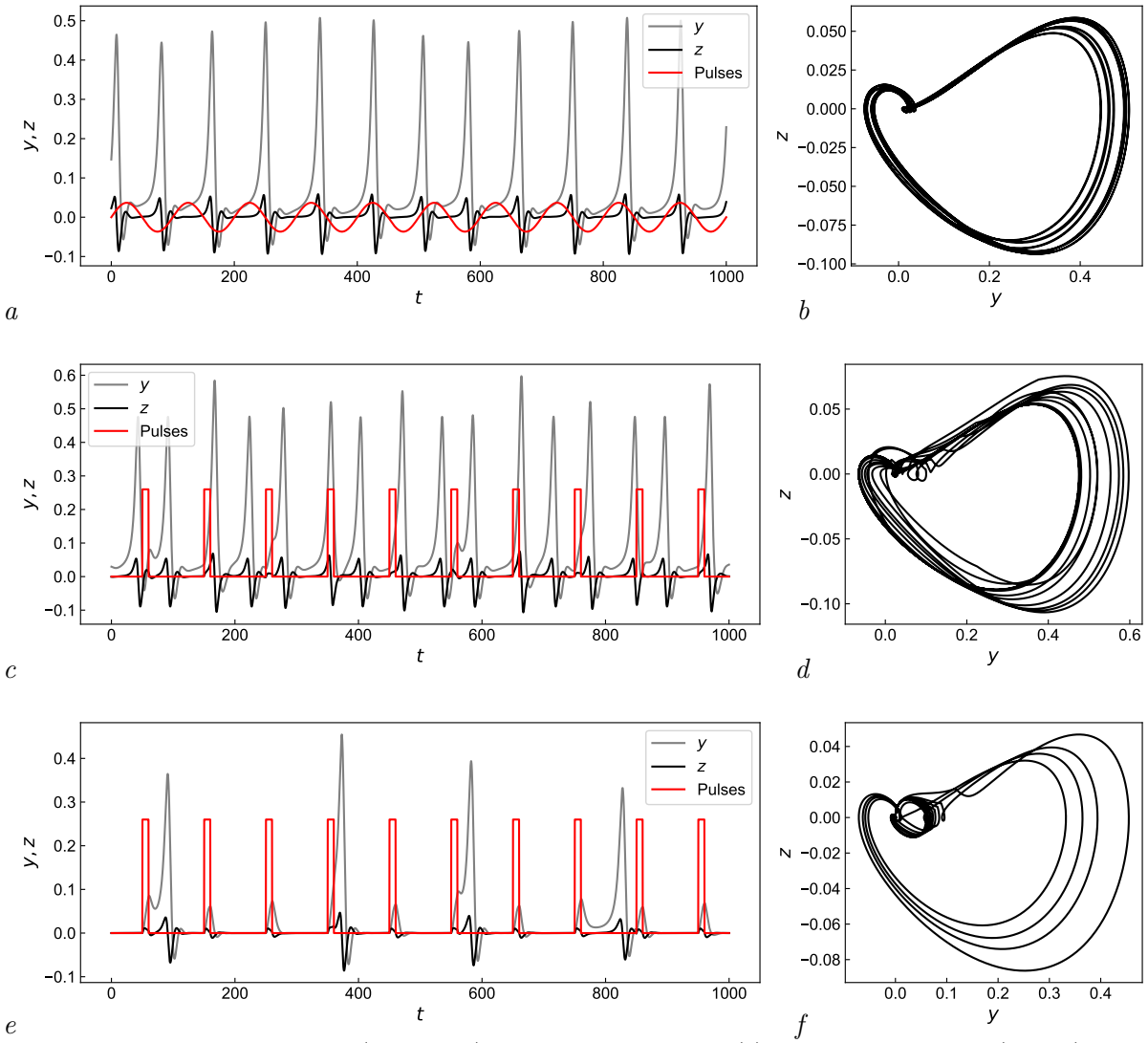

Fig. 1. Time series of variables y (observable) and z from the model (1) and external driving (a, c, e). Phase portraits in the projection (y, z) of the system (1) (b, d, f). Parts a, b correspond to the system under harmonic driving in the oscillatory regime. Parts c, d correspond to the system under square pulse driving in the oscillatory regime. Parts e, f correspond to the system under square pulse driving in the excitable regime

signal was added to all time series. In Fig. 1 time series and phase portraits are given without observation noise. The reconstruction was carried out both in rows with noise and in rows without noise. The following results are given only for rows with noise, unless it is additionally specified, since the method is focused on working with noisy data.

3.2. Reconstruction of PLL parameters. The easiest way to assess the quality of reconstruction is by comparing the recovered values of the effective parameters a_0 and a_1 with the values calculated analytically using the formula (5). For a_0 with pulsed exposure, an additional correction is introduced, caused by a non-zero average of the external impact, which is compensated by an effective change in the parameter g. The reconstruction results for all five modes are shown in Fig. 2. We see that in the oscillatory mode for all three types of impact, the estimates of a_1 turn out to be quite accurate: their relative error does not exceed 2%. For a pulse effect, such accuracy can be achieved already at $K = 3$ — a further increase in the number of harmonics does not lead to a refinement of estimates. For the excitable mode, the relative error of estimates a_1 is greater and is on the order of 4%. At the same time, the best results are achieved when using $K = 5$.

The estimation errors of a_0 are generally significantly higher than a_1. This can be caused by various reasons. One of them is that in the formula (7) this coefficient stands for time, and it is not a bounded variable, unlike y, z and f. Unlimited linear growth of t with an increase in the length of the series is a problem in numerical counting, worsening the statistical characteristics primarily of the estimate a_0. In [19], the main source of errors was the derivative dz/dt. In the modified algorithm described in this paper, there is no need to calculate the second derivative. But due to the integration of the original equation (1), a term containing a linear dependence on time appeared. Therefore, errors in the definition of a_0 in a sense can be considered a payment or compensation for the absence of the need for double numerical differentiation. Another possible reason for the low accuracy of the recovery of the parameter a_0 is the smallness of the value g in the considered modes. This automatically means both the smallness of its contribution to the overall dynamics, and high relative errors of estimates with small absolute ones.

3.3. Reconstruction of external influence. The second important criterion for the success of the reconstruction procedure is the restoration of external influence when using trigonometric polynomials of varying degrees. The results for the oscillatory mode for some used values of the degree of the trigonometric polynomial K are shown in Fig. 3. In numerical

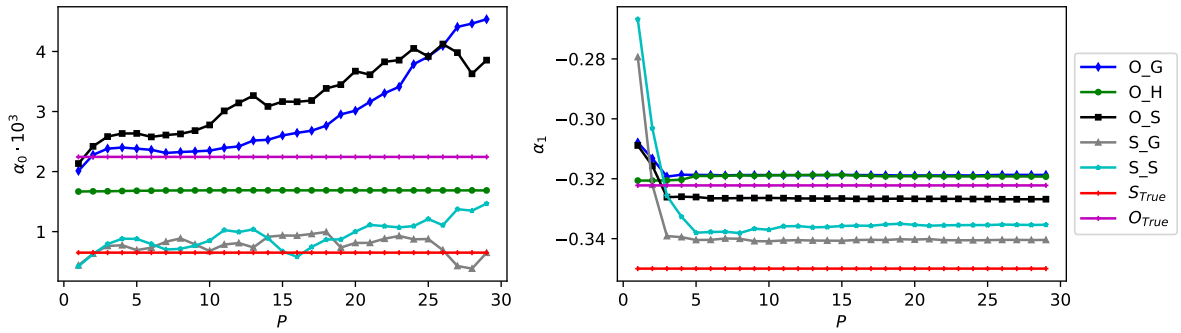

Fig. 2. The dependences of the reconstructed values of the coefficients a_0 and a_1 on the order of the used trigonometric polynomial K. The three curves marked as O (O_G for Gauss pulses, O_H for harmonic driving and O_S for square pulses) belong to the oscillatory regime, the true value for them is indicated by the horizontal line O_{True}. Two curves marked as S (S_G for Gauss pulses, S_S for square ones) belong to the excitable regime, for them the true value is denoted as S_{True}. The value of a_0 is given multiplied by 10^3 for the convenience (color online)

experiments, others were also used: larger and smaller values of K, the results for which are not shown in Fig. 3, so as not to clutter it up.

The harmonic effect is well restored at any K. A significant increase in K relative to the optimal value of $K = 1$ leads only to small distortions of the sine wave, which is clearly seen in Fig. 3, *a*. For Gaussian pulses, $K = 15$ makes it possible to achieve a decent approximation — such that visually the oscillations $I^{\theta}_{\text{ext}}(t)$ inside the period, inevitably present when approximated by a finite trigonometric polynomial, become invisible (Fig. 3, *b* — orange curve corresponding to $K = 5$). The exact approximation of rectangular pulses is theoretically achievable only in the limit. We take into account that they have a vertical front, which means that they contain all frequencies, including infinitely large ones (or at least so large that they are unsolvable at the current sampling frequency). Rice. 3, *c* contains several different variants: the variant at $K = 5$ is very visually similar to the effect of Gaussian pulses reconstructed at the same $K = 5$. Reconstruction at $K = 15$ logically has more local minima on the period, and the oscillation amplitude itself is smaller; there are already two extremes on the pulse itself, and the front is noticeably steeper, which distinguishes it from the approximation of Gaussian pulses. Reconstruction at $K = 25$ already has three highs on the pulse itself and an even steeper front.

The results of the reconstruction of the exposure for the excitable mode (Fig. 4) do not differ qualitatively from what is presented in Fig. 3, *b*, *c* for oscillatory mode. In general, it can be stated that the proposed approach makes it possible to fairly accurately restore the shape of the external periodic effect, while for some types it requires a very high degree of trigonometric polynomial. Interestingly, the accuracy of the approximation of the impact has little effect on the accuracy of the reconstruction of the PLL parameters a_0 and a_1. For example, according to the PLL series, under the influence of rectangular pulses at $K = 5$, the parameter values are restored no worse than at large values, but the effect itself cannot be identified as rectangular.

3.4. Reconstruction of a nonlinear function. The third criterion for the success of the reconstruction — identification of the nonlinear function $f(\mathsf{3})$, which can be calculated by the calculated coefficients a_k using the formula (12). At the same time, it should be understood that the reconstruction of the nonlinear function f is a relatively weak point of the algorithm, since the formula (12) assumes division by y, and values of $y \approx 0$ are often found, especially for excitable mode.

The results of the reconstruction of the nonlinear function for the oscillatory mode are shown in Fig. 5. The results for all three types of exposure are given for $K = 15$. The different number of periods of the reconstructed sine is explained by differences in dynamic modes due to

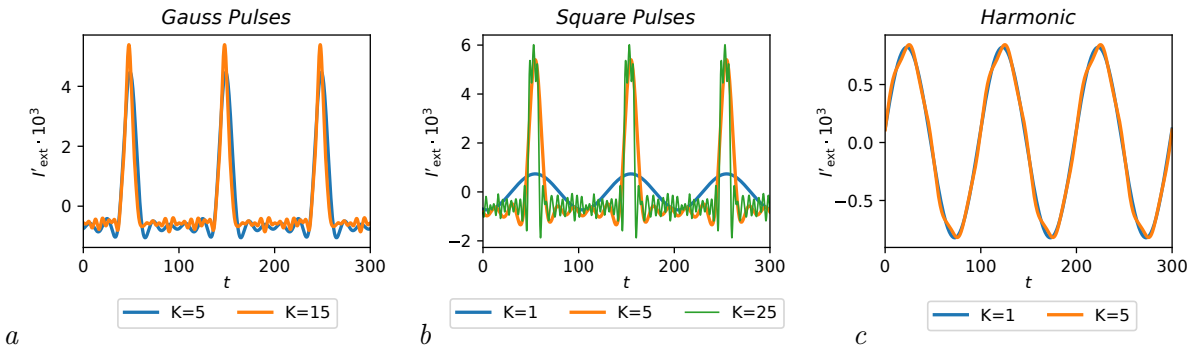

Fig. 3. Reconstructed normalized external driving I^{θ}_{ext} for the oscillatory regime: *a* — Gauss pulses, *b* — square pulses, *c* — harmonic driving. The different curves in each subplot correspond to different orders of the trigonometric polynomial K (color online)

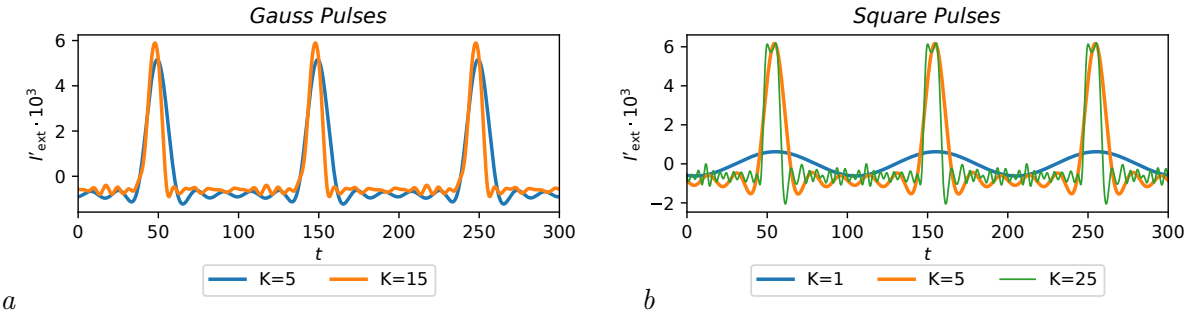

a *b*

Fig. 4. Reconstructed normalized external driving I^{θ}_{ext} for the excitable regime under different driving types: *a* — Gauss pulses, *b* — square pulses. The different curves in each subplot correspond to different orders of the trigonometric polynomial K (color online)

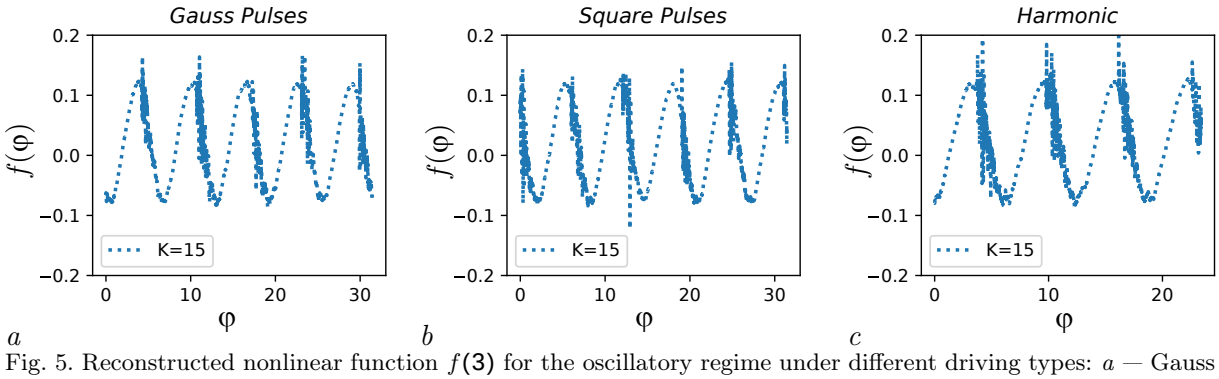

a *b* *c*

Fig. 5. Reconstructed nonlinear function $f(3)$ for the oscillatory regime under different driving types: *a* — Gauss pulses, *b* — square pulses, *c* — harmonic driving. For generality, all results are given for $K = 15$, $m = 151$

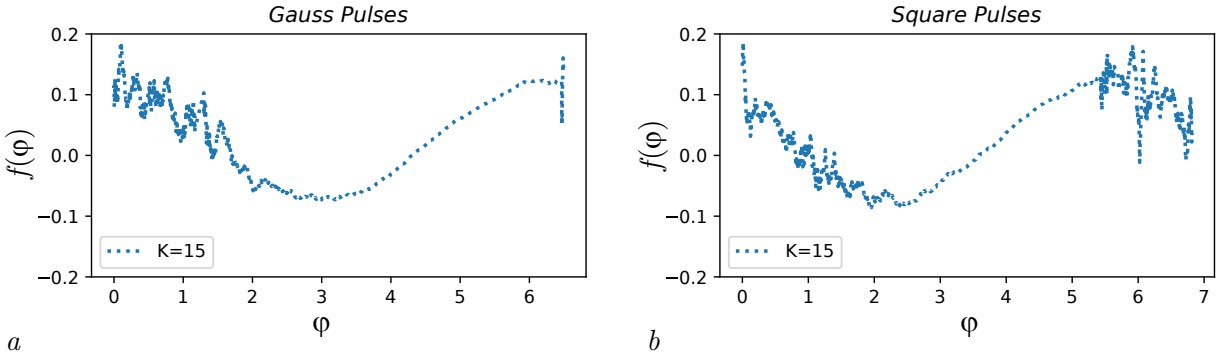

a *b*

Fig. 6. Reconstructed nonlinear function $f(3)$ for the excitable regime under different driving types: *a* — Gauss pulses, *b* — square pulses. For generality, all results are given for $K = 15$, $m = 151$

the presence of exposure — the phase manages to grow by 2p a different number of times during the same observation time. Vertical "noisy"lines from points correspond to state vectors. When $y \approx 0$ there are quite a lot of them in a number due to the peculiarities of the dynamics of the system. To get these results, we had to use a rather significant averaging: $m = 151$. In general, the reconstruction of the nonlinear function is successful: it is possible to restore its periodic character and it looks like a harmonic one.

The results of reconstruction in excitable mode are shown in Fig. 6 for exposure to Gaussian pulses — *a* and rectangular pulses —*b*. All the observed dynamics were focused on one period of the nonlinear function. At the same time, there are significant distortions and the function as a whole is quite noisy. This is due to the long intervals of $y \approx 0$ in this mode. For a significant number of 3, there are no or very few values of y significantly different from zero in the time

series, which leads to errors during reconstruction.

3.5. Selection of the exposure period. So far, all the results have been given for the case when the exposure period of T is known. In reality, of course, this is not the case. At best, the period can be known approximately. However, as the experience of reconstruction of non-autonomous systems [22, 29] shows, even a small error in the definition of T can be very critical, since it quickly leads to the accumulation of a phase shift in time on the main harmonic, and on higher ones — times faster. The easiest way to solve this problem in an experiment is to iterate over the trial T (denote it as $\tilde{T}$). The iteration can be carried out with any reasonable step value $\mathsf{D}\tilde{T}$, since no resampling of values with this step is performed, and the value $\mathsf{W} = 2\mathsf{p}/\tilde{T}$ is used as a multiplier in the formula (7). For simplicity, in the example below, we limited ourselves to a step equal to the sampling step $\mathsf{D}\tilde{T} = \mathsf{D}t$. When choosing a search range, you can focus on the location of local extremes in a smoothed time series (in a noisy series they will stand almost in a row) — it is unlikely that the impact period will be much less than the smallest of them or much more than the largest. In the presented case, the search was performed on the segment $\tilde{T}\ \mathit{2}\ [2; 320]$.

For the most difficult in the approximation of the impact of rectangular pulses, the selection results are — dependence $L(\tilde{T})$ is shown in Fig. 7. Even when using a relatively small degree of the trigonometric polynomial $K = 5$, which does not allow (Fig. 3, *b* and Fig. 4, *b*) satisfactorily describe the shape of the pulse, dependence $L(\tilde{T})$ demonstrates a clear minimum at the value of $\tilde{T} = T = 100$ (see Table), which corresponds to the true value up to $\mathsf{D}t$. The minimum is deep enough, despite the presence of noise. To visualize it, we had to resort to a logarithmic scale. At the same time, an increase in K leads to a deepening not only of the main minimum, but also of its side multiples — $\tilde{T} = 2T$ and $\tilde{T} = 3T$. These side deep minima obviously stem from the possibility of describing the frequency of exposure using the second and third harmonics (while the period is reduced by just 2 or 3 times); this possibility improves with an increase in the degree of the polynomial. The minimum $\tilde{T} = 100$ is always global. For Gaussian pulses, the dependences turned out to be very similar. Only side minima were more pronounced for relatively small K. For harmonic effects, the results did not change significantly when $K > 3$ was changed. When using $K = 1$ and $K = 2$, there were no local extremes on the double and triple (or only triple) values of the period.

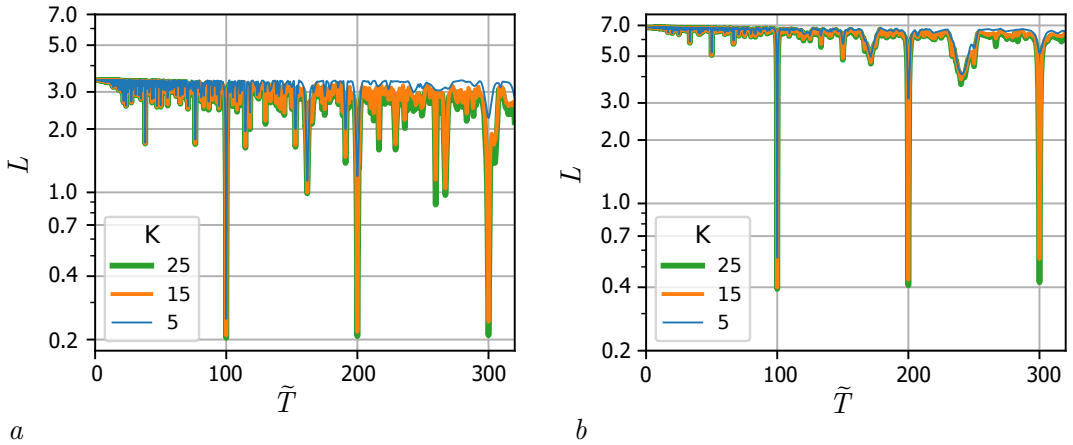

Fig. 7. The dependence of the target function (9) on the trial driving period at reconstruction from time series generated under square pulses using a trigonometric polynomial with order $K = 5$, $K = 15$ and $K = 25$ with smoothing $m = 151$. Fig. *a* corresponds to the oscillatory regime, fig. *b* corresponds to the excitable regime (color online)

Table. Local minima of the target function (9)

	Колебательный режим			Возбудимый режим		
K	$\tilde{T}=100$	$\tilde{T}=200$	$\tilde{T}=300$	$\tilde{T}=100$	$\tilde{T}=200$	$\tilde{T}=300$
25	0.204	0.208	0.210	0.393	0.409	0.423
15	0.210	0.218	0.243	0.400	0.434	0.545
5	0.251	1.195	2.257	0.552	3.148	5.158

The results obtained indicate that when using the approximation of the impact by a trigonometric polynomial, even of a relatively low degree, for the most complex pulses with vertical fronts, it is easy to detect the true value of the impact period according to the dependence of the objective function on the trial period $L(\tilde{T})$ both in oscillatory and excitable mode. The presence of 10% measuring noise cannot interfere with the procedure. Thus, ignorance of the exposure period does not limit the applicability of the method described in the work.

Conclusion

In the works [19,20], approaches have already been proposed to reconstruct the PLL system with a bandpass filter proposed in [14]. They relied, like the algorithm presented in this paper, on an implicit approximation of one of the nonlinear functions of the model; this approach was proposed initially for systems with a delay [18], and then developed for other types of equations, for example, for generalized van der Pol oscillators [31]. The main problem of the solutions proposed in [18,19,31] was that they required numerical calculation of the second derivative. This greatly limits the applicability of the method in the presence of measuring noise: the acceptable noise level is no more than 1-2% from the standard deviation of the signal. How to solve this problem in general is not yet clear. But for a number of systems, the result can be achieved by switching to time-integrated equations, as was shown in [32] for van der Pol and Rayleigh oscillators. The model of the phase-locked frequency system considered in this paper also allows for a similar modification, which we used.

At the same time, the second problem, specific specifically for the reconstruction of the PLL system under consideration, was solved: the sensitivity of the method to the values of the observed one close to zero. In works [19, 20], the state vectors corresponding to $y \approx 0$ were completely excluded from consideration, since in this case the objective function itself was poorly defined. This led to the need to exclude up to half of the entire series in oscillatory modes. And in the excitable mode at $\mathtt{g} = 0$, reconstruction was not carried out at all, since in this mode the values of $y \approx 0$ correspond to most of the time series, as shown in [15, 30]. The algorithm presented here lacks this drawback when reconstructing PLL parameters and external influences. The solution followed from the transition to an integrated system — the corresponding observable variable y left the denominator when determining the nonlinear function of the integrated system and redefining the objective function of the algorithm. At the same time, this modification of the algorithm is not possible for every system, and its applicability depends on the type of equations.

The approximation of the periodic external action was performed by the previously tested for van der Pol oscillators–Toda [22] in a way by decomposition into a trigonometric polynomial. At the same time, the frequency of exposure was selected simply by brute force, and not using a nonlinear optimization algorithm, as in [22], where the Newton method was used, in fact, since the capacities of modern computers allow such an approach. At the same time, there is no probability of the algorithm running away. Such an approximation has shown high efficiency and stability: on the one hand, it is possible to describe a rather complex effect with short pulses of

large borehole close to vertical fronts, on the other hand, even with a significant increase in the number of harmonics beyond the necessary, the method remains stable.

The proposed approach can be directly used for reconstruction from experimental data of a non-autonomous generator described in [17]. At the same time, the presented approach is not suitable for the case of irregular impulse action. It can be assumed that the use of radial basis functions for the approximation of pulses, where a separate function will be associated with each pulse, can partially solve the problem.

References

1. Bezruchko BP, Smirnov DA. Extracting Knowledge From Time Series: An Introduction to Nonlinear Empirical Modeling. Berlin: Springer; 2010. 410 p. DOI: 10.1007/978-3-642-12601-7.
2. Hodgkin AL, Huxley AF. A quantitative description of membrane current and its application to conduction and excitation in nerve. J. Physiol. 1952;117(4):500–544. DOI: 10.1113/jphysiol.1952.sp004764.
3. FitzHugh R. Impulses and physiological states in theoretical models of nerve membranes. Biophysical Journal. 1961;1(6):445–466. DOI: 10.1016/S0006-3495(61)86902-6.
4. Nagumo J, Arimoto S, Yoshizawa S. An active pulse transmission line simulating nerve axon. Proc. IRE. 1962;50(10):2061–2070. DOI: 10.1109/JRPROC.1962.288235.
5. Hindmarsh JL, Rose RM. A model of neuronal bursting using three coupled first order differential equations. Proc. R. Soc. Lond. B. 1984;221(1222):87–102. DOI: 10.1098/rspb.1984.0024.
6. Morris C, Lecar H. Voltage oscillations in the barnacle giant muscle fiber. Biophysical Journal. 1981;35(1):193–213. DOI: 10.1016/S0006-3495(81)84782-0.
7. Gouesbet G, Letellier C. Global vector-field reconstruction by using a multivariate polynomial L_2 approximation on nets. Phys. Rev. E. 1994;49(6):4955–4972. DOI: 10.1103/PhysRevE.49.4955.
8. Packard NH, Crutchfield JP, Farmer JD, Shaw RS. Geometry from a time series. Phys. Rev. Lett. 1980;45(9):712–716. DOI: 10.1103/PhysRevLett.45.712.
9. Baake E, Baake M, Bock HG, Briggs KM. Fitting ordinary differential equations to chaotic data. Phys. Rev. A. 1992;45(8):5524–5529. DOI: /10.1103/PhysRevA.45.5524.
10. Ponomarenko VI, Prokhorov MD. Evaluating the order and reconstructing the model equations of a time-delay system. Tech. Phys. Lett. 2006;32(9):768–771. DOI: 10.1134/S1063785006090100.
11. Ishizaka K, Flanagan JL. Synthesis of voiced sounds from a two-mass model of the vocal cords. Bell. Syst. Tech. J. 1972;51(6):1233–1268. DOI: 10.1002/j.1538-7305.1972.tb02651.x.
12. Barfred M, Mosekilde E, Holstein-Rathlou NH. Bifurcation analysis of nephron pressure and flow regulation. Chaos. 1996;6(3):280–287. DOI: 10.1063/1.166175.
13. Huys QJM, Ahrens MB, Paninski L. Efficient estimation of detailed single-neuron models. Journal of Neurophysiology. 2006;96(2):872–890. DOI: 10.1152/jn.00079.2006.
14. Shalfeev VD. Investigation of the dynamics of a system of automatic phase control of frequency with a coupling capacitor in the control loop. Radiophysics and Quantum Electronics. 1968;11(3):221–226. DOI: 10.1007/BF01033800.
15. Mishchenko MA, Shalfeev VD, Matrosov VV. Neuron-like dynamics in phase-locked loop. Izvestiya VUZ. Applied Nonlinear Dynamics. 2012;20(4):122–130 (in Russian). DOI: 10.18500/0869-6632-2012-20-4-122-130.
16. Matrosov VV, Mishchenko MA, Shalfeev VD. Neuron-like dynamics of a phase-locked loop. The European Physical Journal Special Topics. 2013;222(10):2399–2405. DOI: 10.1140/epjst/e2013-02024-9.
17. Mishchenko MA, Bolshakov DI, Matrosov VV. Instrumental implementation of a neuronlike

generator with spiking and bursting dynamics based on a phase-locked loop. Tech. Phys. Lett. 2017;43(7):596–599. DOI: 10.1134/S1063785017070100.
18. Sysoev IV, Prokhorov MD, Ponomarenko VI, Bezruchko BP. Reconstruction of ensembles of coupled time-delay systems from time series. Phys. Rev. E. 2014;89(6):062911. DOI: 10.1103/PhysRevE.89.062911.
19. Sysoeva MV, Sysoev IV, Ponomarenko VI, Prokhorov MD. Reconstructing the neuron-like oscillator equations modeled by a phase-locked system with delay from scalar time series. Izvestiya VUZ. Applied Nonlinear Dynamics. 2020;28(4):397–413 (in Russian). DOI: 10.18500/0869-6632-2020-28-4-397-413.
20. Sysoeva MV, Sysoev IV, Prokhorov MD, Ponomarenko VI, Bezruchko BP. Reconstruction of coupling structure in network of neuron-like oscillators based on a phase-locked loop. Chaos, Solitons & Fractals. 2021;142:110513. DOI: 10.1016/j.chaos.2020.110513.
21. Lüttjohann A, Pape HC. Regional specificity of cortico-thalamic coupling strength and directionality during waxing and waning of spike and wave discharges. Scientific Reports. 2019;9(1):2100. DOI: 10.1038/s41598-018-37985-7.
22. Smirnov DA, Sysoev IV, Seleznev EP, Bezruchko BP. Reconstructing nonautonomous system models with discrete spectrum of external action. Tech. Phys. Lett. 2003;29(10):824–827. DOI: 10.1134/1.1623857.
23. Mishchenko MA. Neuron-like model on the basis of the phase-locked loop. Vestnik of Lobachevsky University of Nizhni Novgorod. 2011;5(3):279–282 (in Russian).
24. Mishchenko MA, Zhukova NS, Matrosov VV. Excitability of neuron-like generator under pulse stimulation. Izvestiya VUZ. Applied Nonlinear Dynamics. 2018;26(5):6–19 (in Russian). DOI: 10.18500/0869-6632-2018-26-5-6-19.
25. Mishchenko MA, Kovaleva NS, Polovinkin AV, Matrosov VV. Excitation of phase-controlled oscillator by pulse sequence. Izvestiya VUZ. Applied Nonlinear Dynamics. 2021;29(2):240–253 (in Russian). DOI: 10.18500/0869-6632-2021-29-2-240-253.
26. Zhang J, Davidson RM, Wei M, Loew LM. Membrane electric properties by combined patch clamp and fluorescence ratio imaging in single neurons. Biophysical Journal. 1998;74(1):48–53. DOI: 10.1016/S0006-3495(98)77765-3.
27. Jin L, Han Z, Platisa J, Wooltorton JRA, Cohen LB, Pieribone VA. Single action potentials and subthreshold electrical events imaged in neurons with a fluorescent protein voltage probe. Neuron. 2012;75(5):779–785. DOI: 10.1016/j.neuron.2012.06.040.
28. Savitzky A, Golay MJE. Smoothing and differentiation of data by simplified least squares procedures. Anal. Chem. 1964;36(8):1627–1639. DOI: 10.1021/ac60214a047.
29. Bezruchko BP, Smirnov DA. Constructing nonautonomous differential equations from experimental time series. Phys. Rev. E. 2001;63(1):016207. DOI: 10.1103/PhysRevE.63.016207.
30. Sysoev IV, Sysoeva MV, Ponomarenko VI, Prokhorov MD. Neural-like dynamics in a phase-locked loop system with delayed feedback. Tech. Phys. Lett. 2020;46(7):710–712. DOI: 10.1134/S1063785020070287.
31. Sysoev IV. Reconstruction of ensembles of generalized Van der Pol oscillators from vector time series. Physica D. 2018;384–385:1–11. DOI: 10.1016/j.physd.2018.07.004.
32. Sysoev IV, Bezruchko BP. Noise robust approach to reconstruction of van der Pol-like oscillators and its application to Granger causality. Chaos. 2021;31(8):083118. DOI: 10.1063/5.0056901.